Supporting Information for

Combination of On-Chip Field Amplification and Bovine Serum Albumin Sweeping for Ultra-Sensitive Detection of Green Fluorescent Protein

Qiong Pan[†], Meiping Zhao* [†], Shaorong Liu* [‡]

[†] *Beijing National Laboratory for Molecular Sciences, Key Laboratory of Bioorganic Chemistry & Molecular Engineering of Ministry of Education, College of Chemistry and Molecular Engineering, Peking University, Beijing, 100871, China and* [‡] *Department of Chemistry and Biochemistry, The University of Oklahoma, Norman, Oklahoma 73019, USA*

Corresponding authors: mpzhao@pku.edu.cn; shaorong.liu@ou.edu

Theoretical consideration of field amplified pre-concentration and reversed-voltage concentration

At the moment (t_0=0) of voltage switching from the loading step to the pre-concentration step, L_2 is all filled with sample buffer, L_1 and L_3 are filled with running buffer with a short zone of sample buffer to the end of the cross section (Figure 2a). Electric field strengths across L_2 (E_{20}) is described by eq 1.

$$E_{20} = U_2 / l \qquad \text{eq 1}$$

where U_2 is the potential on L_2. After time t_x, the sample zone is pushed back toward S due to EOF, and the length of the sample zone is l_x (see Figure 2b). Then, the electric field strength across L_2 is described by eq 2.

$$E_{2x} = \frac{\gamma U_2}{[(l - l_x) + \gamma l_x]} \qquad \text{eq 2a}$$

$$E_{x0} = \frac{U_2}{[(l - l_x) + \gamma l_x]} \qquad \text{eq 2b}$$

where E_{2x} and E_{x0} are the electric field strength across L_x and (l-l_x), γ is the conductivity ratio of the running buffer and the sample buffer.

Accordingly, bulk flow (V_2) in channel L_2 is the vector sum of the local electroosmotic velocity (V_{eo2}) and the pressure-driven velocity (V_{h2}) in each channel, because of the uneven liquid level between SR and other reservoirs, there exists a hydrodynamic pressure from SR to the intersection. It creates an addictive flow rate (V_{h2}) which adds up to the bulk flow in L_2 (V_{2b}) together with EOF, as expressed in eq3.

$$V_{2b} = V_{eo2} - V_{h2} \qquad \text{eq 3}$$

In addition, there is the pressure-driven velocity usually produced by the imbalance of local EOFs in the low-conductivity sample buffer and the running buffer. However, in our case, the hydrodynamic pressure is much more notable than the back-pressure caused by EOF imbalance, so the pressure-driven velocity is mostly produced by hydrodynamic force, defined as V_{h2}.

Since L_2 is occupied with a sample zone, whose length is L_x, and a running buffer zone, whose length is (l-l_x), V_{eo2} is the average of two parts weighted by the ratios, as described by eq 4.

$$V_{eo2} = (1-\frac{l_x}{l})\mu_{eox0}E_{x0} + (\frac{l_x}{l})\mu_{eo2x}E_{2x} \qquad \text{eq 4}$$

where μ_{eox0} and μ_{eo2x} are the electroosmotic mobility for the running buffer and the sample buffer. If we define $x = \frac{l_x}{l}$, as the ratio of sample zone length in L_2, from eq 2, 3 and 4, the bulk flow in L_2 (V_{2b}) in terms of x can be obtained as in eq 5.

$$V_{2b} = \frac{(1-x)\mu_{eox0} + \gamma x \mu_{eo2x}}{1+(\gamma-1)x} \bullet \frac{U_2}{l} - V_{h2} \qquad \text{eq 5}$$

Because

$$U_i \propto I_i l_i, \quad U_2 + U_3 = V_3 - V_2, \quad U_4 + U_3 = V_3 - V_4$$

where U_i and I_i represent the potential and current on each channel, l_i stands for the length of each channel, and V_i stands for the voltage applied to the reservoir. U_2 can be calculated with voltages on each reservoir and the current on each channel. U_2 under different voltage applied to the reservoir is shown in Table 1.

Under the applied voltage, the negatively charged analyte in the sample buffer has an electrophoretic velocity (V_{ep}=$\mu_{ep}E_{2x}$) and in the direction opposite to EOF. In the two buffer system, the analytes are in low-conductivity buffer with much higher local electric field strength than the high-conductivity buffer. The electrophoretic velocity, V_{ep} of the analyte anions can be expressed as in eq 6.

$$V_{ep} = \mu_{ep}E_{2x} = \frac{\mu_{ep}\gamma}{[(1-x)+\gamma x]} \bullet \frac{U_2}{l} \qquad \text{eq 6}$$

It should be noted that U_2 is a variable depending on x. In this experiment, we monitored the electric current through L_2. It increased initially within the first few seconds and then remained virtually a constant during the FASI, indicating a relatively stable potential along L_2. In order to simplify the calculation, U_2 is assumed to be a constant. Then U_2 can be calculated with the final current in each channel and the voltages applied to each reservoir. The calculated U_2 values are listed in Table S1.

Table S1. U_2 under Different Voltage Applied to Each Reservoir

V_1 (V)	V_2 (V)	V_3 (V)	V_4 (V)	I_1 (mA)	I_2 (mA)	I_3 (mA)	I_4 (mA)	U_2 (V)
1680	1680	2000	0	4.5	4.5	20.5	11.5	76
1620	1620	2000	0	5.0	5.0	21.0	11.0	86
1600	1600	2000	0	5.5	5.5	22.0	11.0	94
1550	1550	2000	0	6.0	6.0	23.0	11.0	100
1510	1510	2000	0	6.5	6.5	24.0	11.0	106

For a given μCE, the voltages applied to all reservoirs and the buffer conductivity ratio was kept constant. In our case, U_2=100 V and γ=20; l=0.50 cm. The electroosmotic mobility for sample solution (2.2 mM Tris base, 2.2 mM tetraborate acid, pH 7.5) and BGE solution (44.5 mM Tris base, 44.5 mM tetraborate acid, pH8.0) are 6.07×10^{-4} and 3.14×10^{-4} cm^2/Vs, respectively. The electrophoretic mobility of GFP in 20-fold diluted TB buffer is 1.35×10^{-4} cm^2/Vs. The bulk velocity driven by the static pressure is 0.09 cm/s. Substituting these values into equations 1a and 1b, V_{2b} and V_{ep} can be expressed as a function of x. V_{2b} and V_{ep} will also change with U_2, as displayed in Figure S1.

A lot of insightful information can be extracted from the relationships presented in Figure S1 for us to understand the concentration approach described in this paper. Referring to eq 5, the bulk solution flow (V_{2b}) consists of the hydrodynamic flow (V_{h2}) and EOF (V_{eo}). V_{h2} is a constant if only the relative liquid levels in all reservoirs are maintained the same. V_{eo}, however, decreases when x decreases. Under certain conditions (see Figure S1b), $-V_{ep}$ curve intersects with V_{2b} curve at a particular x value, indicating that the bulk solution moves in one direction while analyte migrates in the opposite direction but at the same scale. Then $-V_{ep}$ becomes greater than V_{2b} after the intersection, which means the apparent velocity of GFP changes direction. Eventually, V_{eo} and V_{h2} balance one another (at the intersection of V_{eo} and V_{h2} curves, see Figure S1c) and V_{2b} equals to zero. That is, the sample/BGE boundary stays stagnant while the concentrated anion analyte migrates into L_2.

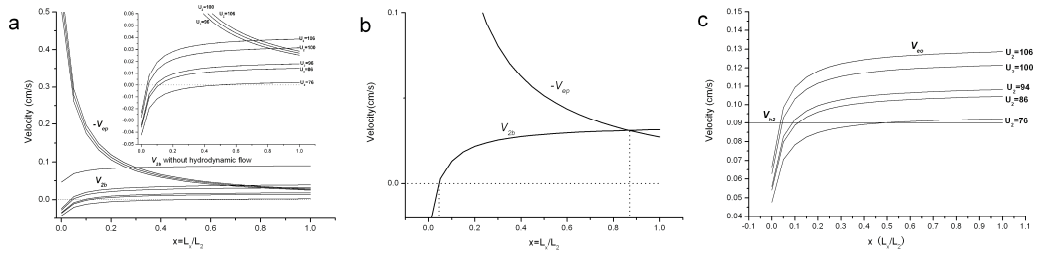

Figure S1. a) Plot of the calculated bulk flow velocities and electrophoretic velocities of GFP during field amplified pre-concentration under different potential along L_2. The inset shows the expanded view of the lower part of the *y* axis. b) Plot of the calculated bulk flow and electrophoretic velocities of GFP when U_2=100V. c) Plot of the calculated electroosmotic flow (V_{eo}) along L_2 and the detected hydrodynamic flow (V_{h2}). Calculation is based on eq 1, channel length of L_2=0.5cm, conductivity ratio γ=20. V_{2b} is the bulk flow velocity in channel L_2, and V_{ep} is the electrophoretic velocity of GFP.

Initially in step 2, the sample/BGE boundary was pushed back, against the hydrodynamic flow, toward SR by EOF. The sample zone was narrowed. In the course of this process, l_x decreased with time. Referring to Figure S1b, the value of x progressed from right to left. When x was at the right-hand side of the intersection, V_{2b}>-V_{ep} and GFP moved in the direction to SR (see Figures 2a and 2b), but due to the different velocity of GFP in the sample zone and the BGE, GFP decelerated and stacked at the sample/BGE boundary. As x went to the left-hand side of the intersection, V_{2b}<-V_{ep} and GFP moved in the direction to channel intersection and GFP in SR also moved into L_2 (see Figures 2c), thus increased the amount of sample injected. When V_{eo}=V_{h2}, sample/BGE boundary and the bulk solution became stagnant while GFP kept migrating into L_2. Because GFP was concentrated moving toward the channel intersection, L_2 was filled with the GFP sample but at a much higher concentration (see Figures 2d and 2e). In our experiment, this step took ~35 seconds.

Guidelines for Voltage Setting in *Step 2*

Depending on the magnitude of the hydrodynamic flow, the voltage on L_2 should be set within an appropriate range to guarantee the balance between the hydrodynamic flow

and EOF. When the EOF and the hydrodynamic flow balance with each other, V_{2b} is zero. So

$$\frac{(1-x)\mu_{eox0}+\gamma x\mu_{eo2x}}{1+(\gamma-1)x}\bullet\frac{U_2}{l}=V_{h2}$$

As we want the stagnant point to be inside L_2, x should be in the range of 0 to 1. So

$$U_2=\frac{V_{h2}\bullet l}{\mu_{eox0}}\quad(x=0)\text{ and }\quad U_2=\frac{V_{h2}\bullet l}{\mu_{eo2x}}\quad(x=1)$$

Entering all the variations, we can get the range of U_2. Referring to Table 2, we can get the appropriate voltage setting. In our case, the voltage setting range was 74~143 V. If the voltage is below 74 V, EOF would not be able to push the sample/BGE boundary toward SR; if the voltage is above 143 V, the hydrodynamic flow would not be able to balance EOF inside the channel.

Video record of the whole concentration process during *Step 2*

A series of fluorescent images of L2 during the concentration process was obtained using a Leica TCS-SP2 Confocal Laser Scanning Microscope (Leica Microsystems, Heidelberg, Germany) with a 488 nm laser at a line scanning frequency of 400 Hz and a 1× objective. These images were assembled into movies using the Leica Confocal software.

In the attached video file (video of *Step2*), the channel on the right side is L_2. At t = 3 s, 2 kV was applied to BR, 1.55 kV was applied to SR and SW, while BW was grounded. This voltage setting created an overall (EOF plus hydrodynamic) flow from BR to all other reservoirs. During t=3~11 s, the sample solution being pushed toward SR by the high conductivity BGE. Due to the conductivity difference between sample solution and BGE, GFP was stacked in the BGE near the sample/BGE boundary. During t=12~18 s, the GFP sample zone moved back toward the intersection and L2 was filled with the concentrated GFP. The excessive sample is removed via L1.

Video record of the whole concentration process during *Step 3 and 4*

To show more detail of the short-period process of step 4, a scan frequency of 800 Hz and a 2× objective were used. The attached video file (video of *Step* 3 and *4*) shows the process during *Step 3* and *4*. The channel on the right side is L_2. From 0 to 15 s, all voltages were turned off, and the concentrated sample zone was allowed to hydrodynamically flow across the intersection to channel L_4, L_2 and L_3. At t = 15 s, the fluorescence intensity at the channel intersection became weak, indicating the concentrated sample has been totally moved out of L_2, so the reversed voltage was turned on. The record from 16 to 22 s corresponds to the reversed-voltage concentration process. The GFP zone in L_4 was pushed to the intersection. At t = 23 s, voltages of 1.60 kV, 1.60 kV and 2 kV were applied to SW, SR and BR, respectively, and BW was grounded as described in Step 5. Then the sample zone at the top end of L_4 was pushed into L_4 and separated.

Reproducibility test results of BSA sweeping

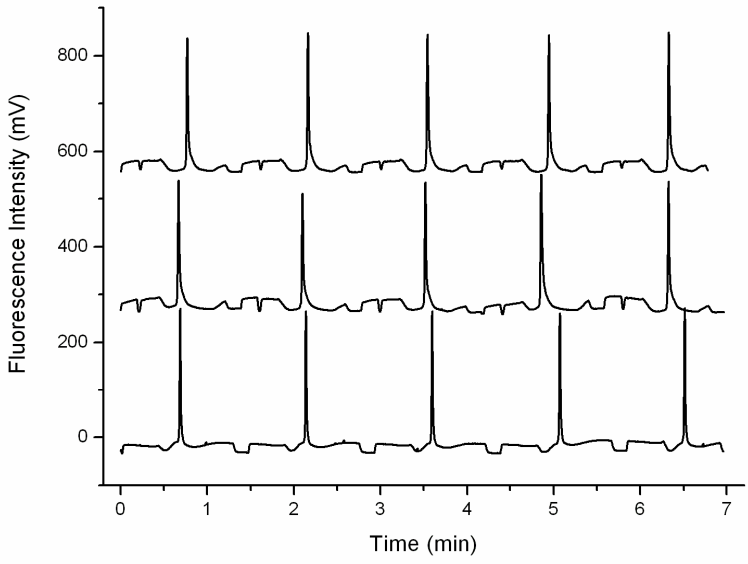

Figure S2. Electrophorograms of three parallel runs of separation, including washing, conditioning the microchip and consecutive 5-step electrophoresis. Each electrophorogram represents for 5 consecutive 5-step electrophoresis in one run.

Further investigation and discussion on the separation of GFP and GFP-IGF-I

For the separation of the mixture sample of GFP and GFP-IGF-I, very sharp GFP peaks were obtained. However, the GFP-IGF-I peak was relatively broad. The isoelectric points of GFP and IGF-I are 5.3 and 8.2, respectively, it is assumed that the fusion protein GFP-IGF-I has a pI value higher than GFP. We have also examined the electrophoresis of only GFP-IGF-I under the same concentration condition (Fig. S3a), it can be seen that the sweeping is pretty effective, although the signal enhancement factor is smaller than that of GFP, which may be caused by the less affinity of BSA with GFP-IGF-I than with GFP. But it can be presumed that with further optimization of the BSA concentration, pH and sweeping length, the signal enhancement factor could be improved. While in the mixture of the two proteins, limited amount of BSA would first interact with GFP, which has more affinity, and GFP-IGF-I could not be swept as effective as it is swept alone. This may explain why the peak of GFP-IGF-I was not as much sharpened as the peak of GFP in the mixture of the two proteins (Fig. S3b). This provides a very interesting aspect of the competition affinity reaction between different proteins. Also, as the channel surface is negatively charged, the peak broadening is presumably also due to the protein adsorption to the channels wall, because GFP-IGF-I may be closer to its neutral state under pH 7.5.

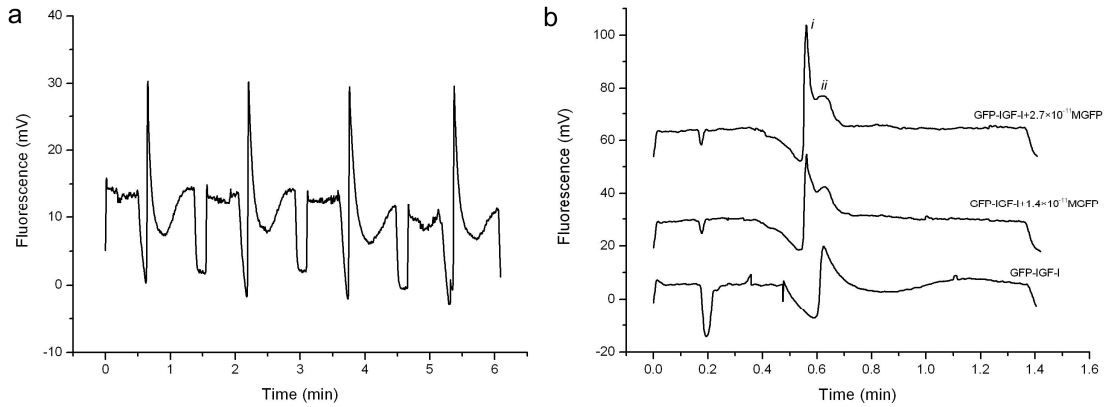

Figure S3. a) Four consecutive electropherograms of GFP-IGF-I. b) Comparison of the electropherograms of GFP-IGF-I mixed with different concentrations of GFP. Based on the peak height, it is deduced that peak *i* corresponds to GFP and peak *ii* corresponds to GFP-IGF-I. Electrophoresis condition: running buffer, TB with 2% BSA; sample buffer, TB.